Analogue modeling results showing fault network evolution during multiphase triaxial strain
(https://doi.org/10.5880/GFZ.FPXO.2025.001)

Jun Liu [1,2], Matthias Rosenau[1], Ehsan Kosari[1], Sascha Brune[1,3], Frank Zwaan[1,4,5], Onno Oncken[1]

1. *GFZ Helmholtz Centre for Geosciences (GFZ), Potsdam, Germany*
2. *Department of Earth Sciences, Freie Universität Berlin, Berlin, Germany*
3. *Institute of Geosciences, University of Potsdam, Germany*
4. *Department of Geosciences, University of Fribourg, Fribourg, Switzerland*
5. *Institute of Earth Sciences, University of Lausanne, Lausanne, Switzerland*

** Corresponding author: junliu@gfz.de*

1. Licence

2. Citation

When using the data please cite:
Liu, J., Rosenau, M., Kosari, E., Brune, S., Zwaan, F., Oncken, O. (2025): Analogue modeling results showing fault network evolution during multiphase triaxial strain. GFZ Data Services. https://doi.org/10.5880/GFZ.FPXO.2025.001

The data are supplementary material to:
Liu, J., Rosenau, M., Kosari, E., Brune, S., Zwaan, F., Oncken, O. (2025): The evolution of fault networks during multiphase triaxial strain: An analogue modeling approach. Journal of Geophysical Research - Solid Earth. https://doi.org/10.1029/2025JB031180

Table of contents

3. Data description

This data set includes the results of high-resolution digital image correlation (DIC) analysis and digital elevation models (DEM) applied to analogue modelling experiments (Table 1). Six generic analogue models are extended on top of a rubber sheet. In Series A, as extension velocity increases, the initial biaxial plane strain condition evolves into triaxial constrictional or intermediate strain. Models A1 and A2 are two-phase models and Model A3 is a three-phase model. Conversely, in Series B, as extension velocity decreases, the model starts with triaxial constrictional strain and ends up with biaxial plane or intermediate triaxial strain. Models B1and B2 are two-phase models and Model B3 is a three-phase model. Detailed descriptions of the experiments can be found in Liu et al. (submitted) to which this data set is supplement. The data presented here are visualized as topography, the horizontal cumulative surface strain, and incremental profiles.

3.1. Monitoring and analysis of experiments

Laboratory: HelTec – Laboratory for experimental tectonics at the GFZ Helmholtz Centre for Geosciences

Digital image correlation techniques (PIV) and Structure from Motion (SfM) are used to monitor surface deformation for all experiments. Digital image correlation techniques (PIV) and Structure from Motion (SfM) are used to monitor surface deformation for all experiments (e.g., Liu et al., 2024, 2024a).

The photogrammetric technique, 'Structure-from-Motion' (SfM) (e.g., Westoby et al., 2012), is used to acquire high-resolution (0.45 mm/pixel) digital elevation models (DEM) at the end of each phase. A consumer-grade digital camera (Canon D810) is deployed to take overlapping top- and oblique view photographs on the surface. These photographs were input to the software Agisoft Photoscan (Metashape) to generate a 3-D point cloud and finally a DEM at high resolution of 0.45 mm/pixel.

All experiments were monitored by a stereoscopic pair of two 12-bit, 50-megapixel monochrome CMOS cameras (LaVision Imager MX50M) at high spatial resolution (6-8 px/mm) and temporal resolution. The temporal resolution depends on extension velocity so that each image can be taken every 1 mm displacement. The recorded images are processed with commercial PIV software LaVision Davis 10.1 allowing to derive the surface topography and full 3-dimensional surface velocity field with high accuracy (≤ 0.1 px) (Adam et al., 2005). Parameters of the DIC processing are reported in Table1.

Table 1: Dem and DIC parameters (LaVision Davis 10.1).

	SfM Processing	***PIV Processing***									
Model ID according to Liu et al.	**DEM resolution** (mm/pixel)	**Monitoring** 2D (one camera)/3D (two	**Pixel scale** (px/mm)	**Monitoring displacement** (mm)	**Correlation mode**	**Increment (mm wall displacement)** (mm)	**Correlation mode**	**Increment (mm wall displacement)** (mm)	**Subset size (px)**	**Step size (px)**	**Calcutaion mode**
Series A: models from biaxial to triaxial strain											
A1	0.45	3D	5.15	1	sum of differential	2	differential	5	51	17	fast
A2	0.45	3D	5.15	1		2		5	51	17	fast
A3	0.45	3D	5.34	1		2		5	51	17	fast
Series B: models from triaxial to biaxial strain											
B1	0.45	3D	5.93	1	sum of differential	2	differential	5	51	17	fast
B2	0.45	3D	5.68	1		2		5	51	17	fast
B3	0.45	3D	6.13	1		2		5	51	17	fast

3.2. Data, data products and software

For all experiments, a Matlab-based script is used to automatically visualize cumulative principal strains and incremental strain (Fig. 1) based on input files. The DIC-derived incremental deformation field was further analyzed by extracting extension (in color) along a profile (indicated in the middle column maps) in increments of 5 mm (0.61% of extension) in sequence, such that the vertical axis corresponds to cumulative extension (~time).

For all experiments, Digital elevation models are displayed by means of cumulative surface maps. A Matlab-based TopoToolbox was deployed to visualize topography maps (Schwanghart & Scherler, 2014).

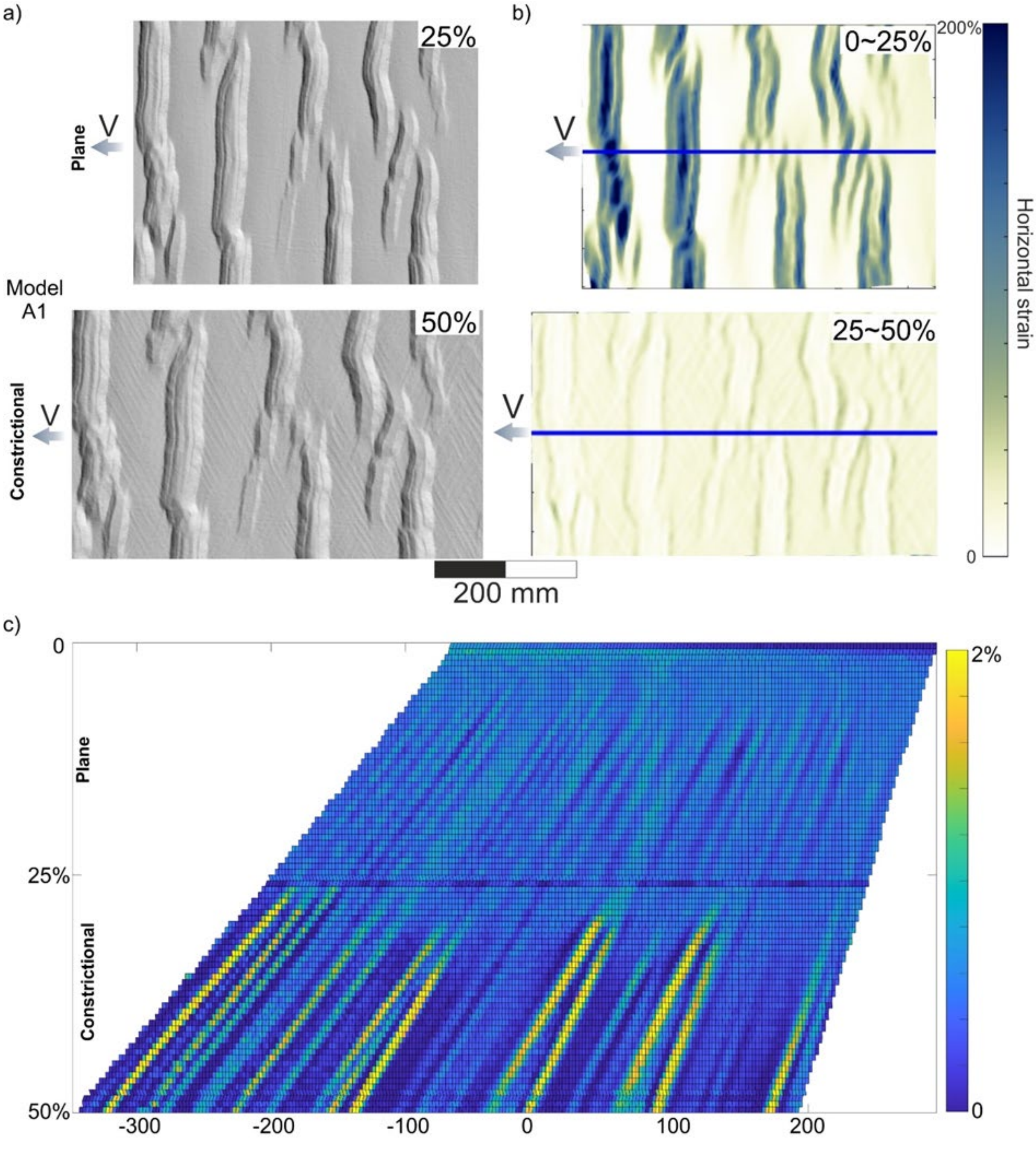

Figure 1: Results of Model A. a) Topographic maps at the end of the individual phase representing finite (cumulative) deformation. B) Maps of surface horizontal strain accumulated during individual phases highlighting faults active in each phase. c) Incremental extension profiles versus extension (~time) visualizing the temporal evolution of strain rate or fault activity. The gray arrows indicate longitudinal extension direction.

4. File description

The folder "2025-001_Liu-et-al_Data.zip" contains three sub-folders (e.g., DEM, Surface strain, and Incremental profiles). For each of the six models of Series A and B, we provide:

(i) **2025-001_Liu-et-al_DEM:** Cropped topography data (finite deformation) at the end of the individual phase in .tif format ("Model ID")

(ii) **2025-001_Liu-et-al_Surface-strain:** PIV-derived cumulative surface strain data during individual phases in .xlsx format as a grid file ("Model ID"). Each file has 3 spreadsheets representing the X_grid, Y_grid and the horizontal strain

(iii) **2025-001_Liu-et-al_Incremental-profiles:** Incremental extension profiles versus extension for series A and B in .csv format

Table 2: Example of Surface strain files. For each model, several Excel tables are provided, each with spreadsheeds for X_grid, Y_grid and horizontal strain. The full list of files is provided in the file "2025-001_Liu-et-al_list-of-files.pdf"

	0-25%			**25-50%**		
2025-001_Liu-et-al_**Model-A1**	X_grid	Y_grid	Horizontal strain	X_grid	Y_grid	Horizontal strain
2025-001_Liu-et-al_**Model-A2**	X_grid	Y_grid	Horizontal strain	X_grid	Y_grid	Horizontal strain
2025-001_Liu-et-al_**Model-B1**	X_grid	Y_grid	Horizontal strain	X_grid	Y_grid	Horizontal strain
2025-001_Liu-et-al_**Model-B2**	X_grid	Y_grid	Horizontal strain	X_grid	Y_grid	Horizontal strain

5. References

Adam, J., Urai, J. L., Wieneke, B., Oncken, O., Pfeiffer, K., Kukowski, N., Lohrmann, J., Hoth, S., van der Zee, W., & Schmatz, J. (2005). Shear localisation and strain distribution during tectonic faulting – New insights from granular-flow experiments and high-resolution optical image correlation techniques. Journal of Structural Geology, 27(2), 283-301, https://doi.org/10.1016/j.jsg.2004.08.008

Liu, J.; Rosenau, M.; Brune, S.; Kosari, E.; Rudolf, M.; Oncken, O. (2024): Fault Networks in Triaxial Tectonic Settings: Analog Modeling of Distributed Continental Extension With Lateral Shortening. Tectonics. https://doi.org/10.1029/2023tc008127

Liu, J., Rosenau, M., Brune, S., Kosari, E., Rudolf, M., & Oncken, O. (2024a). Surface deformation and topography data from analogue modelling experiments addressing triaxial tectonics in regions of distributed extension [Data set]. GFZ Data Services. https://doi.org/10.5880/GFZ.4.1.2024.001

Schwanghart, W., & Scherler, D. (2014). TopoToolbox 2 – MATLAB-based software for topographic analysis and modeling in Earth surface sciences. Earth Surface Dynamics, 2, 1-7. http://doi.org/10.5194/esurf-2-1-2014

Westoby, M. J., Brasington, J., Glasser, N. F., Hambrey, M. J., & Reynolds, J. M. (2012). 'Structure-from-Motion' photogrammetry: A low-cost, effective tool for geoscience applications. Geomorphology, 179, 300-314. http://doi.org/10.1016/j.geomorph.2012.08.021